Current Analytical Chemistry, 2022, *18*, 204-216

RESEARCH ARTICLE

A Fluorene based Fluorogenic "Turn-off" Chemosensor for the Recognition of Cu^{2+} and Fe^{3+}: Computational Modeling and Living-cell Application

Sukriye Nihan Karuk Elmas[1], Duygu Aydin[1], Tahir Savran[1], Eray Caliskan[2], Kenan Koran[3], Fatma Nur Arslan[1], Gokhan Sadi[4], Ahmet Orhan Gorgulu[3] and Ibrahim Yilmaz[1,*]

[1]*Department of Chemistry, Kamil Ozdag Science Faculty, Karamanoglu Mehmetbey University, Karaman, Turkey;* [2]*Department of Chemistry, Science Faculty, Bingol University, Bingol, Turkey;* [3]*Department of Chemistry, Faculty of Science, Firat University, Elazig, Turkey;* [4]*Department of Biology, Kamil Ozdag Science Faculty, Karamanoglu Mehmetbey University, Karaman, Turkey*

Abstract: ***Background*:** The traditional methods for the detection and quantification of Cu^{2+} and Fe^{3+} heavy metal ions are usually troublesome in terms of high-cost, non-portable, time-consuming, specialized personnel and complicated tools, so their applications in practical analyses is limited. Therefore, the development of cheap, fast and simple-use techniques/instruments with high sensitivity/selectivity for the detection of heavy metal ions is highly demanded and studied.

***Methods*:** In this study, a fluorene-based fluorescent "turn-off" sensor, methyl 2-(2-((((9H-fluoren-9-yl)methoxy)carbonyl)amino)-3- phenylpropanamido) acetate (probe **FLPG**) was synthesized *via* one-pot reaction and characterized by ^{1}H-NMR, ^{13}C-APT-NMR, HETCOR, ATR-FTIR and elemental analysis in detailed. All emission spectral studies of the probe **FLPG** have been performed in CH_3CN/HEPES (9/1, v/v, pH=7.4) media at rt. The quantum (Φ) yield of probe **FLPG** decreased considerably in the presence of Cu^{2+} and Fe^{3+}. The theoretical computation of probe **FLPG** and its complexes were also performed using density functional theory (DFT). Furthermore, bio-imaging experiments of the probe **FLPG** was successfully carried out for Cu^{2+} and Fe^{3+} monitoring in living-cells.

***Results*:** The probe **FLPG** could sense Cu^{2+} and Fe^{3+} with high selectivity and sensitivity, and quantitative correlations (R^2>*0.9000*) between the Cu^{2+}/Fe^{3+} concentrations (0.0−10.0 equiv). The limits of detection for Cu^{2+} and Fe^{3+} were found as 25.07 nM and 37.80 nM, respectively. The fluorescence quenching in the sensor is managed by ligand-to-metal charge transfer (LMCT) mechanism. Job's plot was used to determine the binding stoichiometry (1:2) of the probe **FLPG** towards Cu^{2+} and Fe^{3+}. The binding constants with strongly interacting Cu^{2+} and Fe^{3+} were determined as 4.56×10^{8} M^{-2} and 2.02×10^{10} M^{-2}, respectively, *via* the fluorescence titration experiments. The outcomes of the computational study supported the fluorescence data. Moreover, the practical application of the probe **FLPG** was successfully performed for living cells.

***Conclusion*:** This simple chemosensor system offers a highly selective and sensitive sensing platform for the routine detection of Cu2+ and Fe3+, and it keeps away from the usage of costly and sophisticated analysis systems.

Keywords: Fluorescence sensor, fluorene, iron, copper, DFT, bio-imaging.

ARTICLE HISTORY

Received: October 02, 2020
Revised: January 12, 2021
Accepted: February 02, 2021

DOI:
10.2174/1871520621666210322112005

1. INTRODUCTION

Recently, research has focused on the design and development of fluorescent chemosensors to detect environmentally and biologically important heavy metal ions. When the products contaminated with these metal ions are consumed as foodstuff or drinking water, it is obvious that it will damage humans by disrupting the balance of the body [1-4]. Among the heavy metal ions, copper (II) (Cu^{2+}) and iron (III) (Fe^{3+}) are considered essential trace ions for organisms, and they play vital roles in many biological reactions [5,6]. However, the accumulation of these ions in the food chain, their non-biodegradable properties and their excessive intake causes a serious threat to human health [5].

Copper is a crucial and third plentiful element for living organisms, and it has the most important responsibilities in numerous essential biochemical reactions [5-9]. An excessive or inadequate copper intake to the human body (permis-

*Address correspondence to this author at the Department of Chemistry, Kamil Ozdag Science Faculty, Karamanoglu Mehmetbey University, P.O. Box: 70100, Karaman, Turkey; Tel/Fax: ++0-338-226-2151, +0-338-226-2150; E-mail: iyilmaz@kmu.edu.tr

1875-6727/22 $65.00+.00

sible level is 10-12 mg/per day for adults by WHO, average maximum level in the blood is 100-150 μg/dL) can lead to various neurodegenerative disorders and serious diseases. An excessive accumulation of copper in the body is quite toxic and causes some critical diseases, such as Alzheimer's, Parkinson's and Wilson diseases [10,11]. On the other hand, an inadequate intake of copper gives rise to Menkes and cardiovascular diseases, also copper deficiency anemia disease [10,12-14]. Iron is another essential and second abundant element for almost bio-organisms, and it plays main roles in a number of fundamental metabolic and physiological pathways, including DNA/RNA synthesis, proton/electron transfers, co-factor role in enzyme synthesis, transportation of oxygen, *etc*. [7,15,16]. As a result of iron deficiency or excessive iron intake, many health problems can occur in the body (*permissible level in water is at 0.3 mg* L^{-1}*, approximately 6 μM, by WHO*) [7,15]. The deficiency of iron causes anemia, liver or kidney damage, and diabetes. However, the excessive intake of iron can result in hemochromatosis, Alzheimer's and Parkinson's disease, *β*-thalassaemia and cancer [6,11,15,17-20].

Due to the adverse effects of heavy metal ions on the human health, developing new analytical methods for the detection and quantification of heavy metal ions, particularly Cu^{2+} and Fe^{3+}, in real samples have been regarded as significant research [1,2,5]. So far, a variety of analytical techniques, such as atomic absorption/emission spectroscopy (AAS/AES), inductively coupled plasma-mass/atomic emission spectrometry (ICP-MS/AES), gas chromatography (GC) and plasmon resonance-Rayleigh scattering (PR-RS) spectroscopy have extensively been utilized to detect the trace levels of Cu^{2+} and Fe^{3+} [1,2,5,6]. Nevertheless, these traditional methods are usually troublesome in terms of high-cost, non-portable, time-consuming, specialized personnel and complicated tools, so their applications in practical analyses are limited [1,7]. Therefore, the development of cheap, fast and simple-use techniques with high sensitivity/selectivity for the detection of heavy metal ions is highly demanded and studied.

In recent years, the fluorescent sensing systems have received great attention in heavy metal analyses [21,22] with widespread applications owing to their many advantages, such as excellent sensitivity and selectivity [23-25], quick response time, cost-free equipment, on-site monitoring and easy-operation [1,6,7]. Considering these advantages, up to now, numerous studies that focused on the design and development of novel fluorogenic chemosensors for Cu^{2+} and Fe^{3+} sensing have been reported [5,15,17,26]. Within this framework, a large number of fluorogenic chemosensors based on BODIPY [27], coumarin [8], indole [4], rhodamine [17], phosphazene [15], antracene [6], pyrene [9], and fluorine [5] derivatives have been developed for the monitoring of Cu^{2+} and Fe^{3+}. For example, in recent years, by Li and co-workers, a novel rhodamine-cyanine based Cu(II) and Fe (III) selective bifunctional NIR ratiometric colorimetric and fluorescent probe was produced and employed in $MeCN/H_2O$ and $MeOH/H_2O$ with a detection limits of 10.2×10^{-5} M for Cu^{2+} and 7.37×10^{-5} M for Fe^{3+}, respectively [16]. Zhang *et al*. described a new and dual-response fluorescent sensor based on quinoline and benzimidazole, which could be used for the recognition of Cu^{2+} and Fe^{3+} in the range of 10^{-7} M in 100 % aqueous medium (50 mM Tris buffer, pH 7.2) [28]. Additionally, Zhu *et al*. developed a new and tri-responsive fluorescent Schiff base probe ((E)-2-((4-(diethylamino)benzylidene)amino)benzoic acid, DBAB) for the "turn-off" determination of Fe^{3+}, Fe^{2+} and Cu^{2+}, simultaneously. This sensor exhibited a suitable selectivity for the target ions in DMF within 10^{-6} M detection limits [29]. However, only a few simple and effective fluorogenic probes have been reported for the detection of Cu^{2+} and Fe^{3+}, and therefore the development of new probes for multiple ion recognition with a single sensor due to its advantages such as cost-free and more efficient analyses [5], is still a great need.

In the present study, we synthesized a fluorene-based methyl 2-(2-((((9H-fluoren-9-yl)methoxy) carbonyl) amino)-3- phenylpropanamido) acetate (probe **FLPG**), and then the fluorogenic characteristics and mechanism of the probe **FLPG** were investigated in CH_3CN/HEPES (9/1, v/v, pH=7.4) media. The experimentally observed results of the probe **FLPG** have been well supported by theoretical calculations. Furthermore, in living-cell applications, the probe **FLPG** exhibited a perfect sensing performance towards Cu^{2+} and Fe^{3+} with nano-molar detection limits.

2. EXPERIMENTAL SECTION

2.1. Chemicals

All chemicals and solvents (analytical or spectroscopic grade) were purchased from different commercial suppliers and were utilized without further purification. All stock solutions of metal salts ($1\times10^{2-}$ M) as perchlorates of Cu^{2+}, Fe^{3+}, Cr^{3+}, Sr^{2+}, Cd^{2+}, Al^{3+}, Zn^{2+}, K^{+}, Ba^{2+}, Mg^{2+}, Mn^{2+}, Hg^{2+}, Fe^{2+}, Co^{2+}, Pb^{2+}, Ni^{2+} and Ca^{2+} were prepared in CH_3CN media.

2.2. Apparatus

A Perkin Elmer infrared (IR) spectrometer (Spectrum-100, Perkin Elmer Inc., MA, Wellesley, USA) was employed to record the spectra with attenuated total reflectance (ATR) accessory, and the data were in the range of 4000−650 cm^{-1}. ^1H and ^{13}C-APTand HETCOR NMR spectra were measured in DMSO-d_6 on a Bruker-DPX 400 MHz spectrometer (Bruker, Massachusetts, CA, USA). The CHNS-932 Elementary Chemical Analyzer system (LECO, St Joseph, USA) was used for elemental analysis. Cary Eclipse fluorescence spectrophotometer (Agilent Technologies, Inc., Santa Clara, CA, USA) was employed to conduct fluorescence analyses. All fluorescence studies were carried out at rt with a 1.0 cm path-length quartz cuvette. pH measurements were done using a benchtop pH metre (Mettler Toledo, Zaventem, The Netherlands).High-quality pure water with a resistivity of 18.2 $M\Omega\cdot cm^{-1}$ was freshly obtained from Milli-Q®IQ 7003/05/10/15 water purification machine (MERCK KGaA, Darmstadt, Germany).

2.3. Synthesis of Probe FLPG

The starting materials **Fmoc-Phe-OH** (3.0 g; 7.74 mmol), glycine methyl ester hydrochloride salt (972.18 mg; 7.74 mmol) and 2-chloro-4,6-dimethoxy-1,3,5-triazine (CDMT) (1.50 g; 8.52 mmol) were taken into the dried one-

neck reaction flask. Afterwards, acetonitrile (50 mL) was added to the reaction flask and stirred continuously at rt. Then, N-methyl morpholine (2.13 mmL; 19.36 mmol) was added dropwise to the obtained slurry mixture. The reaction progress was monitored by thin-layer chromatography (TLC) by the mixture of ethyl acetate:hexane (4:5, v/v). The obtained solid in the reaction flask was filtered, and then the solvent was evaporated under a vacuum. The obtained oily product was dissolved in ethyl acetate (30 mL) and filtrated to remove unsolved particles. The ethyl acetate part was extracted with HCl (1.0 N) and $NaHCO_3$ (%5), respectively, and then the organic layer was dried with $MgSO_4$. After filtration of $MgSO_4$, the solvent was removed, and the obtained oily product was dissolved in chloroform (10 mL) and precipitated in hexane.

A white colored solid (**Fmoc-Phe-Gly-OCH$_3$**) (probe **FLPG**) obtained (2.45 g, 70%). Elemental analysis result of $C_{27}H_{26}N_2O_5$ (MW: 458.51), calculated: C, 70.73; H, 5.72; N, 6.11; Found C, 70.79; H; 5.77; N, 6.17%. FT-IR (ATR, cm^{-1}): 3299, 3319 ν_{N-H}, 3028-3064 $\nu_{C-H(Ar)}$, 2853, 2887, 2918 $\nu_{C-H(Alph.)}$, 1647, 1696, and 1737 $\nu_{C=O}$, 1542 $\nu_{C=C}$. ^{1}H-NMR (400 MHz, DMSO-d_6): δ 2.78-2.84 and 3.04-3.08 (2H, H^{12}), 3.65 (3H, s, H^{21}), 3.90-3.98 (2H, H^{19}), 4.10-4.19 (3H, m, H^2 and H^3), 4.28-4.34 (1H, H^{11}), 7.20-7.22 (1H, t, H^{16}), 7.26-7.43 (6H, m, H^6, $H^{14,15}$), 7.40-7.45 (2H, t, H^7), 7.63-7.68 (2H, H^8), 7.74-7.76 (1H, H^{10} (-NH)), 7.88-7.90 (2H, d, H^5), and 8.57-8.60 (1H, t, H^{18} (-NH)).^{13}C-APT-NMR (DMSO-d_6): δ 156.28 C^1, 66.13 C^2, 47 C^3, 144.18 C^4, 120.55 C^5, 125.76 C^6, 128.09 C^7, 127.52 C^8, 141.12 C^9, 56.49 C^{11}, 37.89 C^{12}, 138.68 C^{13}, 128.52 C^{14}, 129.70 C^{15}, 126.71 C^{16}, 172.66 C^{17}, 41.10 C^{19}, 170.71 C^{20} and 52.2 C^{21}.

2.4. Spectroscopic Studies of the Probe FLPG Towards Cu^{2+} and Fe^{3+}

For fluorescence measurements, a stock solution of the probe **FLPG** (10.0 mM) was freshly prepared in CH_3CN and diluted to the concentration of 5.0 μM. Fluorescence spectra were recorded in the region of 280−600 nm (λ_{em}=312 nm, λ_{ex}=272 nm) at rt, and slit widths were 10.0 nm. For the fluorescence titration studies, designated equivalents (0.0−10.0 equiv.) of the Cu^{2+} or Fe^{3+} solutions were added into the probe solution in a 1.0 cm path-length quartz cuvette. The final volumes were adjusted to 3 mL by adding the solution of HEPES buffer, and the final concentration of the probe **FLPG** is 5.0 μM in CH_3CN/HEPES (9/1, v/v, pH=7.4) solution. After equilibrium at room temperature for 1 min (for Cu^{2+} and Fe^{3+} detection), their fluorescence spectra were obtained at λ_{em}=312 nm. For the selectivity studies, the spectra were recorded in the absence and in the presence of different competing metal ions (Cr^{3+}, Sr^{2+}, Cd^{2+}, Al^{3+}, Zn^{2+}, K^+, Ba^{2+}, Mg^{2+}, Mn^{2+}, Hg^{2+}, Fe^{2+}, Co^{2+}, Pb^{2+}, Ni^{2+} and Ca^{2+}), including Cu^{2+} or Fe^{3+} in CH_3CN/HEPES (9/1, v/v, pH=7.4) media.

2.5. Cytotoxic Effects of the Probe FLPG and Metal Ions Over HepG2 Cells

Cell growth inhibitory potential of the probe **FLPG** and its target metals, Cu^{+2} and $Fe^{+3,}$ were investigated over human hepatocellular carcinoma (HepG2) cells obtained from ATCC (ATCC® HB-8065) company. The cells were grown in high glucose DMEM media supplemented with 10% FBS, L-glutamine and penicillin/streptomycin at 37°C with 5% CO_2 and 95% moisture. Cellular toxicity of the probe **FLPG** and metal ions were studied with 2,3-bis-(2-methoxy-4-nitro-5-sulfophenyl)-2H-tetrazolium-5-carboxanilide (XTT) *in vitro* cellular toxicity assay according to our optimized protocol. Briefly, $5x10^{+4}$ cells were seeded in the wells of the 96-well cell culture plate and allowed for cell attachment for 4-hrs. Subsequently, different amounts of the probe **FLPG** and metal ions (10 - 250 μM) prepared in growing media were added to the cells, and they were incubated for 24-hrs. After the addition of 25 μl of activated XTT solution (1 mg/mL) and 2-hrs incubation period, the intensities of the formazan were measured at 450 nm with Multiscan™ GO Microplate Spectrophotometer (Thermo Scientific, USA). Non-linear regression analysis was utilized to calculate IC_{50} values with GraphPad Prism 6.0 software.

2.6. Cell Imaging Studies

The practical applicability of the probe **FLPG** for Cu^{+2} and Fe^{+3} sensing, fluorescent imaging experiments were carried out using HepG2 cell lines. Accordingly, the HepG2 cells were incubated with 50 μM of the probe **FLPG** prepared with 10% DMSO in growth media for one hour. After removal of the probe and washing with PBS three times, the equimolar concentration of cupric and ferric ions was applied to the adherent cells separately for another one hour. Before and after probe and metal ion applications, blue fluorescent, and bright field phase-contrast images of the cells were obtained using a fluorescent cell imaging system (ZOE, Bio-Bad, Germany). The bright field and fluorescent images were merged with the software of the imaging device.

2.7. Theoretical Computation of Probe FLPG and its Complexes

All geometry optimizations were carried out with the Gaussian-09 software-package (Gaussian, Inc., Wallingford CT, UK) using density functional theory (DFT) computations. All geometries were fully optimized in the gas-phase without any restrain using Becke's three-parameter hybrid exchange functional (B3) and the Lee-Yang-Parr correlation functional (LYP) (B3LYP) along with 6-31g(d) basis set [30-34]. Gaussview 5.0.8 software was employed for visualizations of the optimized structures and HOMO-LUMO energy levels.

3. RESULTS AND DISCUSSION

3.1. Fabrication and Characterization of the Probe FLPG

The Fmoc-Phe-Gly-OCH_3 (probe **FLPG**) was synthesized by the reaction of Fmoc-Phe-OH and Gly-OMe.HCl *via* 2-chloro-4,6-dimethoxy-1,3,5-triazine methodology [35,36]. The formation of Fmoc-Phe-Gly-OMe was obtained *via* reaction of N-protected amino acid with amino side free amino acid ester in the presence of 2-acyloxy-4,6-dimethoxy-1,3,5-triazine and N-methyl morpholine as a catalyst. The reaction starts with the nucleophilic attack of NMM to triazine reagent to give a tetrahedral intermediate, and then it turns to dimethyl triazine methyl morpholine (DMTMM) intermediate. Oxygen of carboxylic acid attacks

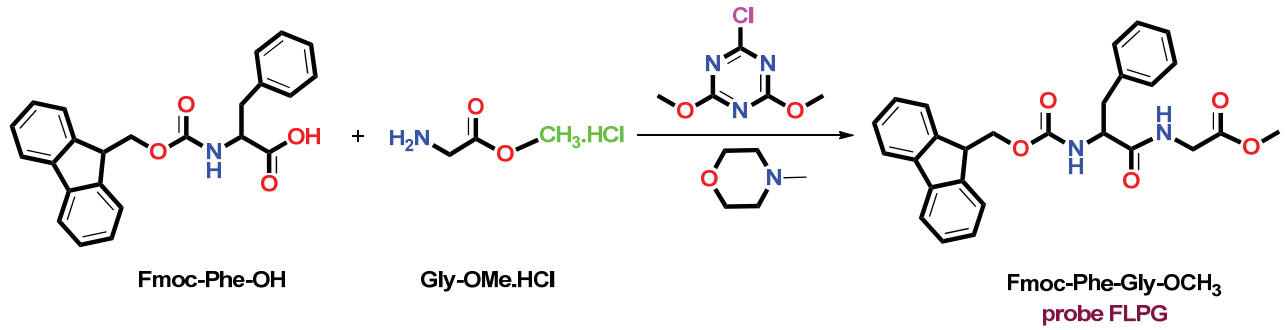

Scheme 1. Synthetic route of the probe FLPG.

the electrophilic carbon atom of intermediate DMTMM, which gives another unstable tetrahedral intermediate that triazine gains its aromaticity and expel NMM to give activated ester compound. In the final step, the amino group of amino acid ester attacks to the electrophilic carbonyl of activated ester to give the target compound **(Fmoc-Phe-Gly-OCH$_3$)** (Scheme **S1**). The reaction mixture was purified *via* acidic work-up. The general synthesis procedure is depicted in Scheme **1**.

FT-IR, elemental analysis, ^{1}H, ^{13}C-APT and HETCOR NMR techniques were used for the characterization of compounds (Fig. **S1-S4**). In the infrared spectrum of probe **FLPG**, three characteristic carbonyl stretching peaks at 1647, 1696, and 1737 cm^{-1}, N-H stretching peaks of two amide bond at 3299, 3319 cm^{-1}, peaks of aromatic stretching vibrations at 3028 and 3064 cm^{-1} show that the structure was formed. The absence of the carboxylic acid O-H stretching peak of the starting material has also supported the formation of the product. In the ^{1}H-NMR spectrum, the presence of the peaks of aliphatic CH_2 proton of glycine at 3.90-3.98 ppm and CH_3 proton of methyl ester at 3.65 ppm indicated that the amino acid reacted with the probe **FLPG**. Another evidence for the product formation was that the existence of the total number of aromatic proton peaks between 7.20-7.90 ppm. The enantiotopic CH_2 protons of phenylalanine resonance at 2.78-2.84 ppm and 3.04-3.08 ppm and the aliphatic protons (H^2 and H^3) of Fmoc group at 4.10-4.19 ppm were proved the formation of the target product.

In the ^{13}C-APT-NMR spectra of probe **FLPG**, the peaks at 66.13, 56.49, 52.2, 47.00, 41.10 and 37.89 ppm of amino acids, the aliphatic carbon peaks of the fmoc group, the carbonyl carbon peaks at 156.28, 172.66 and 172.66 ppm (C^1, C^{17} and C^{20}) and aromatic carbon peaks could be presented as other evidence of the product formation. The exact position of protons and attached carbons were determined by HETCOR-NMR spectrum (Fig. **S4**). The probe **FLPG** has then utilized for the detection of metal ions as a fluorogenic chemosensor in CH_3CN/HEPES (9/1, v/v, pH=7.4) media.

3.2. Fluorescence Studies of the Probe FLPG Towards Cu^{2+} and Fe^{3+}

In the initial stage of the fluorescence experiments, the impact of solvent on the intensity of the probe **FLPG** was tested (Fig. **S5**). When the probe **FLPG** was dissolved in various pure-organic solvent systems (*dimethylsulfoxide, dimethylformamide, tetrahydrofuran, acetonitrile and ethanol*), the maximum intensity was observed in the acetonitrile system. After the addition of Cu^{2+} and Fe^{3+}, the maximum fluorescent quenching was observed in the acetonitrile solution under UV light. Also, CH_3CN-H_2O mixtures with different ratios were studied to construct the probe **FLPG** more utilizable for livings, and it was approved that the 9/1 (v/v) mixture of CH_3CN-H_2O was the most appropriate for fluorescence studies.

To study the pH effect on the fluorescence property of the probe **FLPG**, the emission intensities were measured at different pH values (pH from 4 to 10) in CH_3CN-HEPES (9/1, v/v) media (Fig. **S6**). The emission of the probe **FLPG** and its complexes (**FLPG**-Cu^{2+} and **FLPG**-Fe^{3+}) were not affected within the pH range of 4-10; therefore, pH of the sensing medium was herein adjusted to 7.4 with the favorable buffer solution, HEPES, for livings.

To study the fluorescence sensing properties of probe **FLPG** (5.0 μM) towards a series of metal ions (Cu^{2+}, Fe^{3+}, Cr^{3+}, Sr^{2+}, Cd^{2+}, Al^{3+}, Zn^{2+}, K^+, Ba^{2+}, Mg^{2+}, Mn^{2+}, Hg^{2+}, Fe^{2+}, Co^{2+}, Pb^{2+}, Ni^{2+} and Ca^{2+}), the same volume of 10 equiv perchlorate salts of these ions were individually added into the probe **FLPG** solution. Their fluorescence responses in CH_3CN/HEPES (9/1, v/v, pH=7.4) media were recorded and presented in Fig. **1**. As is illustrated in Fig. **1**, the emission intensity of probe **FLPG** was considerably quenched at 312 nm (λ_{ex}=272 nm) with the adding of Cu^{2+} (23 fold) and Fe^{3+} (20 fold), but other metal ions had not any impact on the intensity of probe **FLPG**. The probable explanation could be due to the fact that the electronic structures of transition metal ions have uncoupled d-electrons while alkaline (group IA) and alkaline-earth (group IIA) metal ions have a blocked-shell electron configuration [37]. These outcomes showed that the probe **FLPG** is more selective to Cu^{2+} and Fe^{3+} than other metal ions and could operate as a fluorescent chemosensor in CH_3CN/HEPES (9/1, v/v, pH=7.4) media.

To estimate the quantitative sensing capability of probe **FLPG** towards Cu^{2+} and Fe^{3+}, the fluorescence titration study was performed. For these experiments, the Cu^{2+} or Fe^{3+} solution was added incrementally (0.0-10.0 equiv) to the solution of probe **FLPG** (Fig. **2**) in CH_3CN/HEPES (9/1, v/v, pH=7.4) media, and the spectra were recorded after each addition. As depicted in Fig. **2a** and **2b**, the emission intensities were significantly quenched at 312 nm with the consecutive addition of responding metal ion (Cu^{2+} or Fe^{3+}) into the solution of probe **FLPG**. This phenomenon is related to the formation of **FLPG**- Cu^{2+} and **FLPG**- Fe^{3+} complexes.

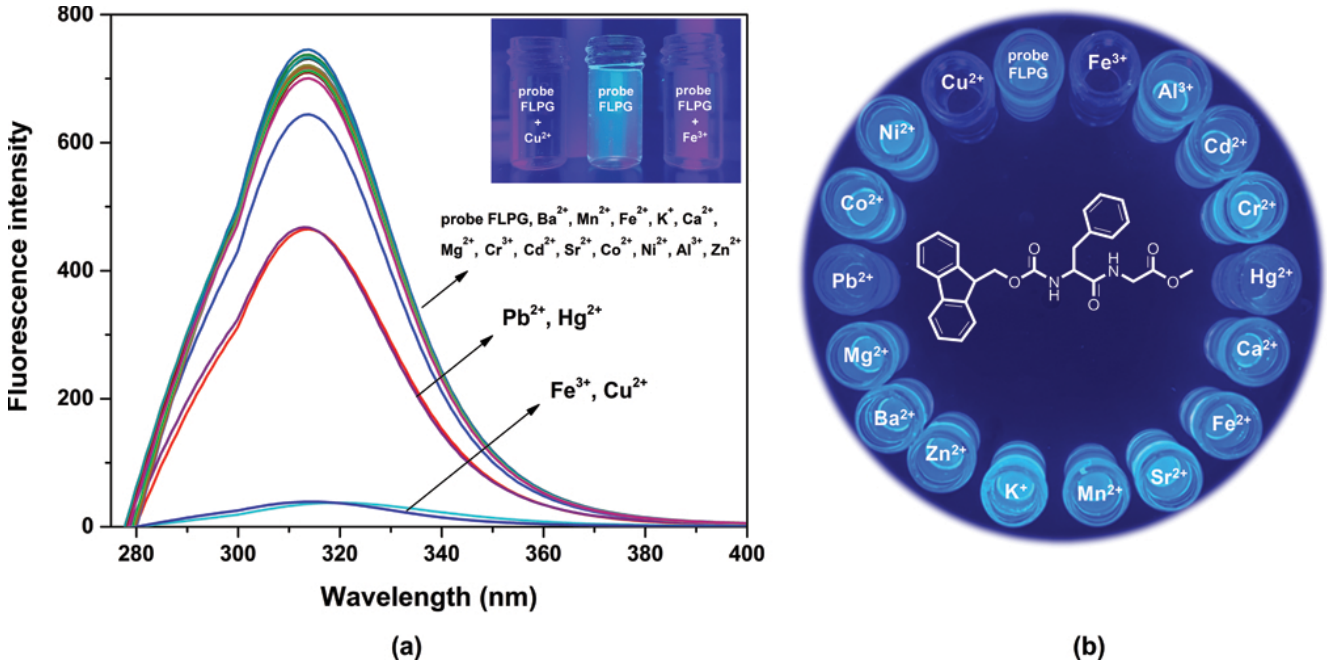

Fig. (1). (a) Fluorescence emission intensity changes of the probe **FLPG** (5.0 μM) with the addition of 10.0 equiv different metal ions (Cu^{2+}, Fe^{3+}, Cr^{3+}, Sr^{2+}, Cd^{2+}, Al^{3+}, Zn^{2+}, K^{+}, Ba^{2+}, Mg^{2+}, Mn^{2+}, Hg^{2+}, Fe^{2+}, Co^{2+}, Pb^{2+}, Ni^{2+} and Ca^{2+}) in CH_3CN/HEPES (9/1, v/v, pH=7.4) media at rt (λ_{em}=312 nm, λ_{ex}=272 nm), **(b)** Fluorescence images of the probe **FLPG** (5.0 μM) with the addition of different metal ions (10.0 equiv) under UV light. (*A higher resolution / colour version of this figure is available in the electronic copy of the article*).

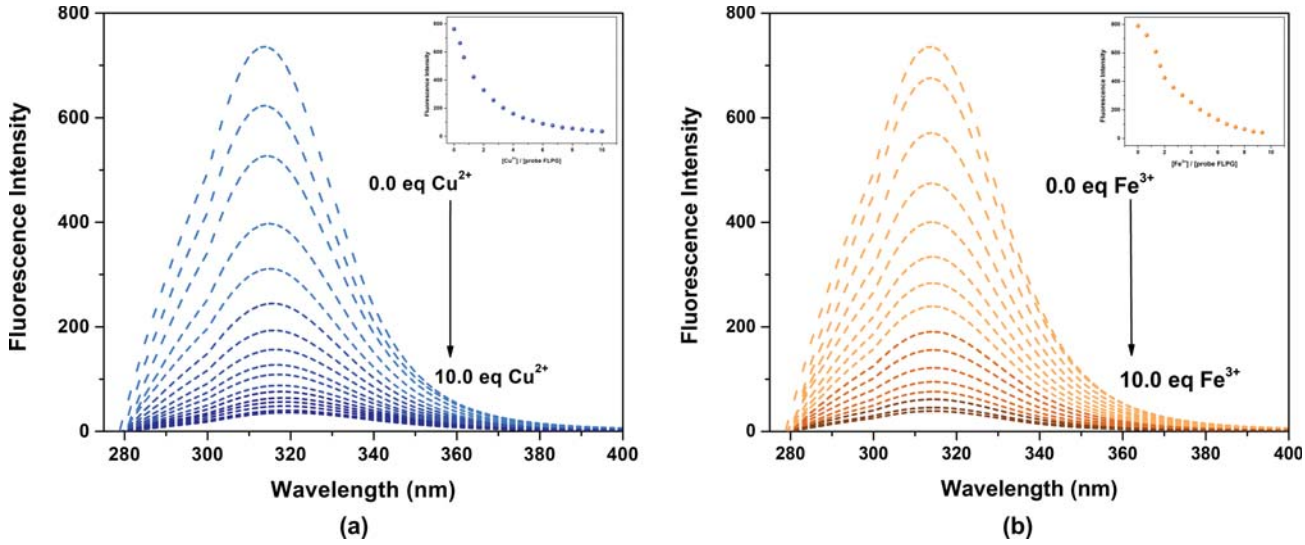

Fig. (2). Fluorescence emission intensity changes of the probe **FLPG** (5.0 μM) with the addition of different concentrations (0.0 -10.0 equiv) of **(a)** Cu^{2+} and **(b)** Fe^{3+} in CH_3CN/HEPES (9/1, v/v, pH=7.4) media at rt (λ_{em}=312 nm, λ_{ex}=272 nm). (*A higher resolution / colour version of this figure is available in the electronic copy of the article*).

The time-dependent emission intensities of probe **FLPG** in the presence of responding metal ion were studied for Cu^{2+} and Fe^{3+}, respectively (Fig. **S7**). The fluorescence quenching values of probe **FLPG** (312 nm) reached the maximum in one minute after the addition of Cu^{2+} or Fe^{3+} in CH_3CN/HEPES (9/1, v/v, pH=7.4) media at rt (λ_{em}=312 nm, λ_{ex}=272 nm). The fluorescence quick response demonstrates that the probe **FLPG** has a great potential for the detection of Cu^{2+} and Fe^{3+} in practical applications.

Based on the fluorescence titration experiments, the detection limits (3σ/K) [38,39] of probe **FLPG** for Cu^{2+} and Fe^{3+} were found to be 25.07 nM and 37.80 nM, respectively (Fig **3a**), and these values were far below the standards in drinking water reported by WHO and EU-WFD guidelines (max. 31.50 μM for Cu^{2+} and 5.37 μM Fe^{3+}) [15,40]. In addition, for numerous biological samples, these detection limits are quite satisfactory, demonstrating the potential usefulness of the proposed sensing platform in trace-level analysis. Moreover, the quantum (Φ) yield studies for the probe **FLPG** and its complexes with Cu^{2+} and Fe^{3+} were carried out at different concentrations in CH_3CN/HEPES (9/1, v/v, pH=7.4) media at rt. The **FLPG**-Cu^{2+} (Φ=0.0035) and

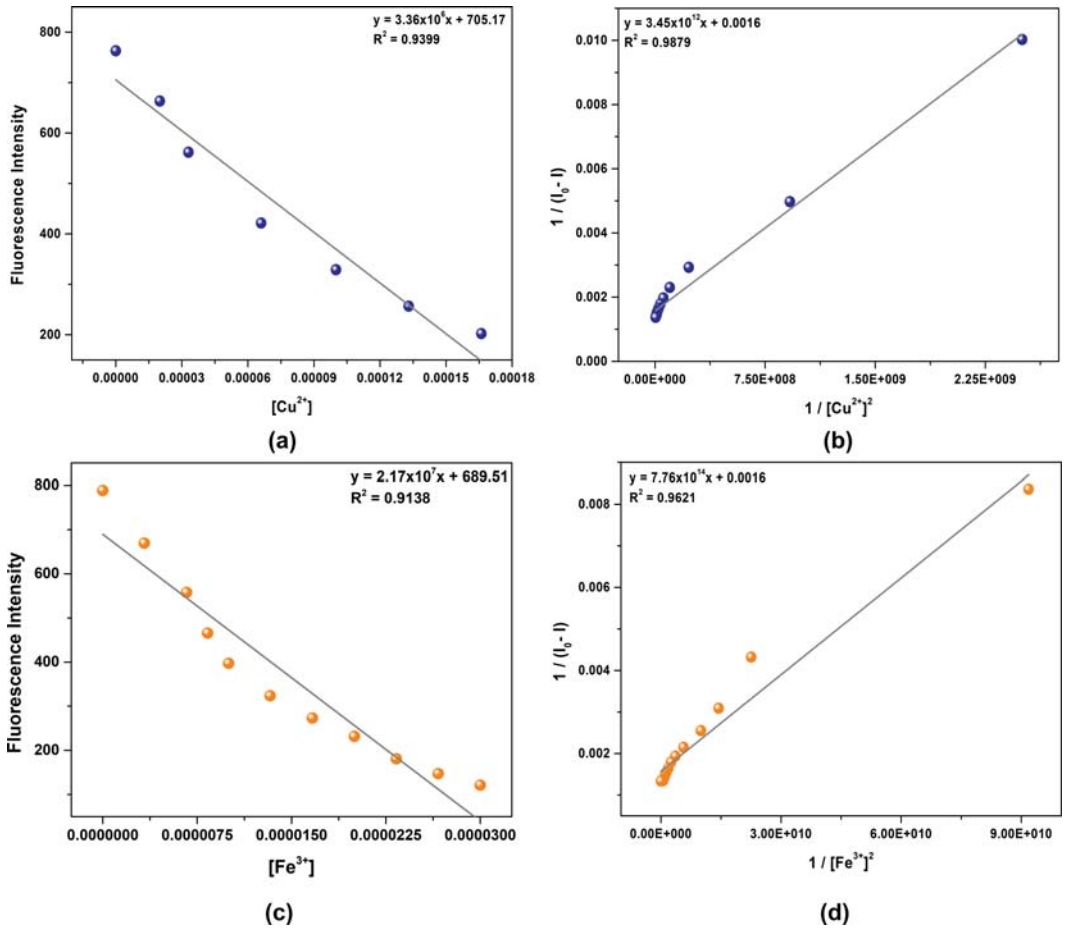

Fig. (3). (a) The quantitative calibration curve of the association between the emission intensities of probe **FLPG** and Cu^{2+} concentrations; **(b)** Benesi-Hildebrand curve of 1/[Cu^{2+}] vs 1/(I_0-I) based on stoichiometry (**FLPG-Cu^{2+}** complex, 1:2); **(c)** the quantitative calibration curve of the association between the emission intensities of probe **FLPG** and Fe^{3+} concentrations and **(d)** Benesi-Hildebrand curve of 1/[Fe^{3+}] vs 1/(I_0-I) based on stoichiometry (**FLPG-Fe^{3+}** complex, 1:2), in CH_3CN/HEPES (9/1, v/v, pH=7.4) media at rt (λ_{em}=312 nm, λ_{ex}=272 nm). (*A higher resolution / colour version of this figure is available in the electronic copy of the article*).

FLPG-Fe^{3+} (Φ=0.0114) complexes demonstrated about 122 and 37 times lower Φ yield than the probe **FLPG** (Φ=0.4300) (Fig. **S8**). The binding constants were also calculated to be 4.56×10^8 M^{-2} for **FLPG-Cu^{2+}** system and 2.02×10^{10} M^{-2} for **FLPG-Fe^{3+}** system from linear curve fitting of the titration data (Fig. **3b** and **3d**) according to the Benesi-Hildebrand equation [41,42]. The worth of probe **FLPG** was confirmed by comparing with the sensing performance of the reported chemosensors (Table **1**), which obviously revealed that the probe **FLPG** could be a highly sensitive fluorogenic chemosensor for the detection of Cu^{2+} and Fe^{3+}.

For deeply studying the selectivity of the probe **FLPG** towards Cu^{2+} and Fe^{3+}, a number of competition experiments were performed, and their emission spectra of the probe **FLPG** solution in the presence of Cu^{2+} or Fe^{3+} and other competing metal ions were recorded (Fig. **4a** and **4b**). The other possible competing metal ions, including Cr^{3+}, Sr^{2+}, Cd^{2+}, Al^{3+}, Zn^{2+}, K^{+}, Ba^{2+}, Mg^{2+}, Mn^{2+}, Hg^{2+}, Fe^{2+}, Co^{2+}, Pb^{2+}, Ni^{2+} and Ca^{2+} with the same equivalent (10.0 equiv) were separately added into the solution of probe **FLPG**, followed by the addition of responding metal ions (Cu^{2+} or Fe^{3+}). As seen in Fig. **4**, the complexes of **FLPG-Cu^{2+}** and **FLPG-Fe^{3+}** showed obvious quenching of fluorescence, as mentioned above, even in the presence of other competing metal ions. Based on the results of these experiments, it is remarkable that no other metal ions influenced the detection of Cu^{2+} and Fe^{3+} by the probe **FLPG** in CH_3CN/HEPES (9/1, v/v, pH=7.4) media, and the probe **FLPG** was a promising fluorogenic chemosensor for multiple ion recognition with a single probe.

3.3. Binding Stoichiometry of the Probe FLPG Towards Cu^{2+} and Fe^{3+}

To establish the possible binding stoichiometry between the probe **FLPG** and responding metal ions, Job's plot method [46] was employed based on the fluorescence titration data (Fig. **5**). As seen in Fig. **5**, the maximum emission intensities at 312 nm were reached when the molar fractions were 0.33 (inflection point), which revealed that the possible binding stoichiometries between the probe **FLPG** and responding metal ions (Cu^{2+} and Fe^{3+}) were both 1:2.

The fluorescence quenching mechanisms of the **FLPG**-Cu^{2+} and **FLPG**-Fe^{3+} complexes were presented in Scheme **2**. For these complex sensing systems, the fluorescence quenching may be due to the ligand-to-metal charge transfer

Table 1. Relative study of the sensing performance of probe FLPG with some reported studies for the fluorogenic detection of Cu^{2+} and Fe^{3+}.

Probe	Solvent System	LOD (M)	Binding Constant (M^{x})	Cell Imaging	Refs.
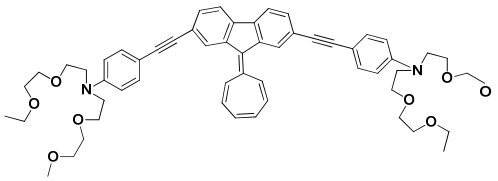	CH_3CN	-	3.1×10^5 (for Cu^{2+}) 1.6×10^5 (for Fe^{3+})	no	[43]
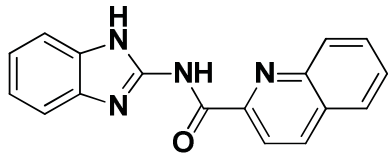	tris buffer (pH 7.2)	1.35×10^{-7} M (for Cu^{2+}) 1.24×10^{-7} M (for Fe^{3+})	8.6×10^4 (for Cu^{2+}) 5.1×10^4 (for Fe^{3+})	yes	[28]
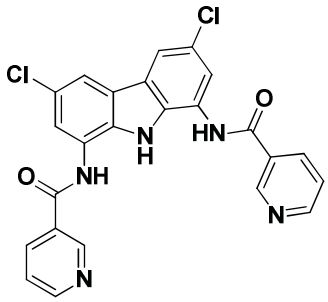	tris-HCl (0.01M DMSO/H_2O, 1:1, v/v, pH=7.4)	-	3.3×10^3 (for Cu^{2+}) 1.5×10^4 (for Fe^{3+})	no	[44]
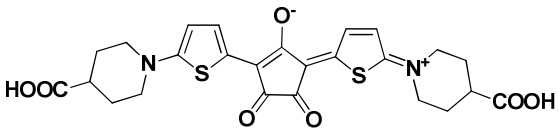	$EtOH/H_2O$ (4/1, v/v)	-	5.58×10^4 (for Cu^{2+}) 2.12×10^4 (for Fe^{3+})	no	[2]
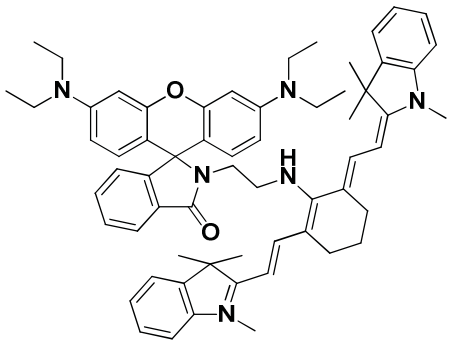	CH_3CN/H_2O (1/1, v/v) (for Cu^{2+}) MeOH /H_2O (1/4, v/v) (for Fe^{3+})	10.2×10^{-5} M (for Cu^{2+}) 7.37×10^{-5} M (for Fe^{3+})	-	yes	[16]
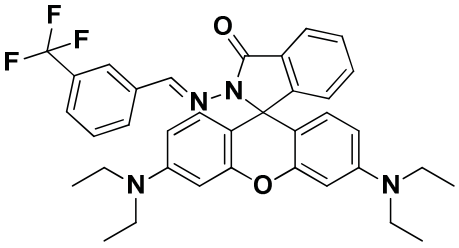	EtOH	5.26×10^{-7} M (for Cu^{2+}) 4.6×10^{-9} M (for Fe^{3+})	1.80×10^3 (for Cu^{2+}) 7.32×10^4 (for Fe^{3+})	no	[45]
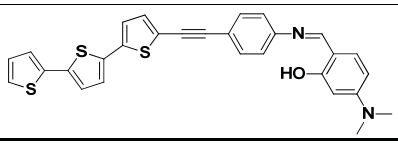	THF/H_2O (7/3, v/v)	5.26×10^{-7} M (for Cu^{2+}) 4.6×10^{-9} M (for Fe^{3+})	1.96×10^5 (for Cu^{2+}) 1.93×10^5 (for Fe^{3+})	no	[7]

(Table 1) Contd….

Probe	Solvent System	LOD (M)	Binding Constant (M^{-x})	Cell Imaging	Refs.
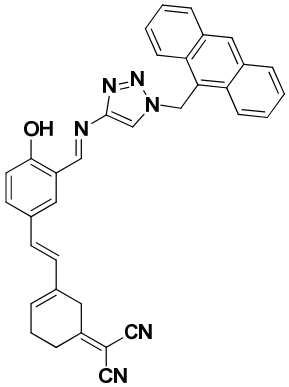	DMSO/H_2O (8/2, v/v)	30.1×10^{-9} M (for Cu^{2+}) 87.3×10^{-9} M (for Fe^{3+})	0.42×10^{3} (for Cu^{2+})	no	[6]
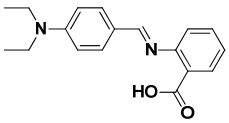	DMF	2.48×10^{-6} (for Cu^{2+}) 2.17×10^{-6} (for Fe^{3+})	3.93×10^{5} (for Cu^{2+}) 3.82×10^{5} (for Fe^{3+})	no	[29]
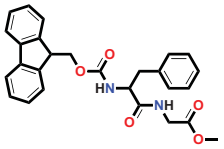	CH_3CN/HEPES (9/1, v/v, pH=7.4)	25.07×10^{-9} (for Cu^{2+}) 37.80×10^{-9} (for Fe^{3+})	4.56×10^{8} (for Cu^{2+}) 2.02×10^{10} (for Fe^{3+})	yes	this work

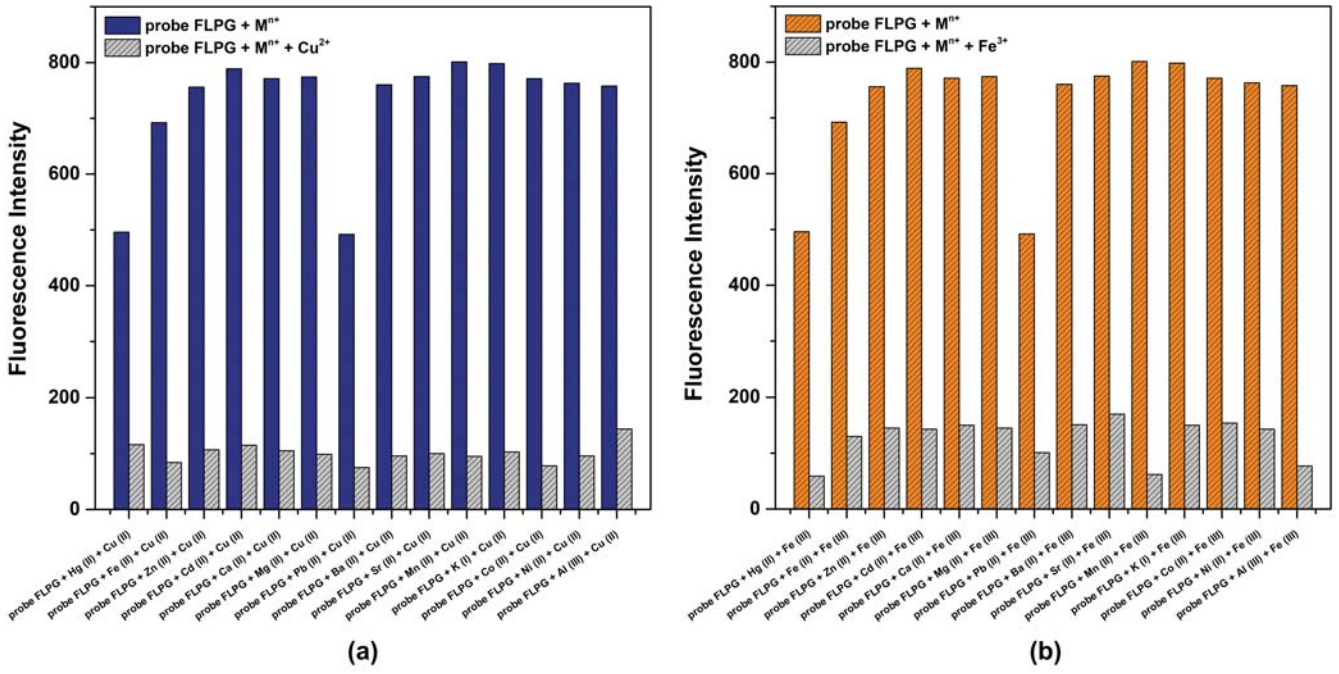

Fig. (4). Selectivity of the probe **FLPG** (5.0 μM) toward **(a)** Cu^{2+} (10.0 equiv) and **(b)** Fe^{3+} (10.0 equiv) and other competing metal aions (10.0 equiv) in CH_3CN/HEPES (9/1, v/v, pH=7.4) media at rt (λ_{em}=312 nm, λ_{ex}=272 nm). (*A higher resolution / colour version of this figure is available in the electronic copy of the article*).

(LMCT) between the probe **FLPG** and paramagnetic target metal ions (Cu^{2+} and Fe^{3+}). That is, the fluorescence of probe **FLPG** was quenched was attributed to form **FLPG**-Cu^{2+} and **FLPG**-Fe^{3+} complexes, the molecule of probe **FLPG** and target ions was close-connected in a complex structure, and the paramagnetic properties of target ions efficiently quenched the emission. This phenomenon is because of the unpaired d-electrons of Cu^{2+} and Fe^{3+}, the electron transfer between the excited states of N and O atoms, and the d-orbitals of these ions occurred.

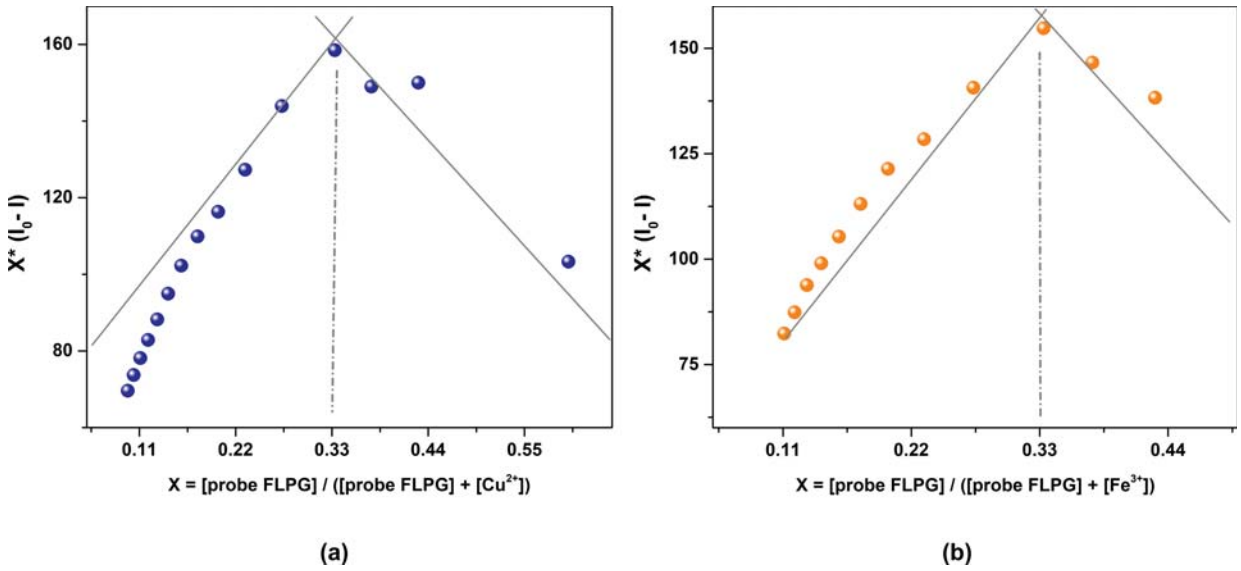

Fig. (5). Job's plots for the complexation of probe **FLPG** with **(a)** Cu^{2+} and **(b)** Fe^{3+} in CH_3CN/HEPES (9/1, v/v, pH=7.4) media at rt, indicating the formation of a 1:2 complexes (λ_{em}=312 nm, λ_{ex}=272 nm). (*A higher resolution / colour version of this figure is available in the electronic copy of the article*).

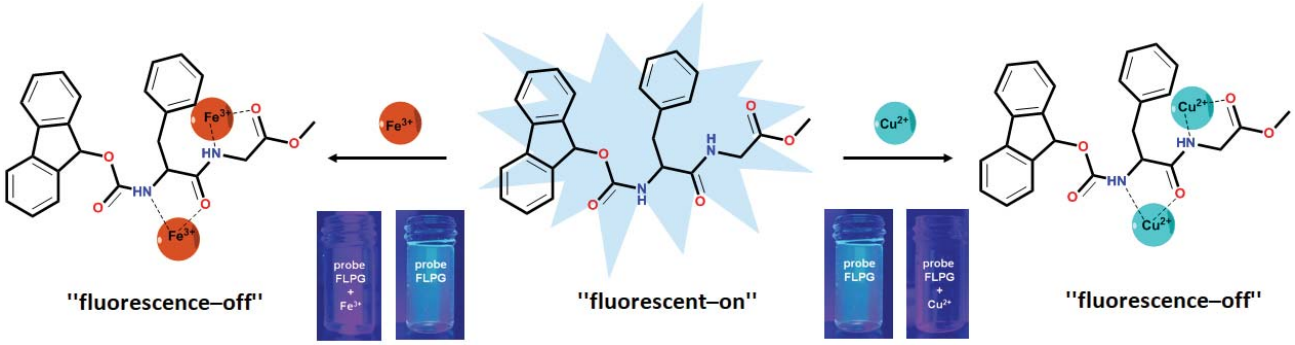

Scheme 2. Fluorescence quenching mechanisms of the **FLPG**-Cu^{2+} and **FLPG**-Fe^{3+} complexes. (*A higher resolution / colour version of this figure is available in the electronic copy of the article*).

3.4. Theoretical Calculation

Computational studies of the characteristics of chemosensor molecules are very precious to analysts. The density functional theory (DFT) calculation is commonly used for forecasting the most reactive site in σ - and π-electron schemes and clarifying a number of reactions in conjugated systems. Herein, the DFT calculations were performed in the gas-phase to propose the probable molecular structure of the probe **FLPG** and its complexes (**FLPG**-Cu^{2+} and **FLPG**-Fe^{3+}), as well as the mechanism of the sensor. The computations for geometry optimizations were done by employing the Gaussian-09 software program (Gaussian, Inc., Wallingford CT, UK) without any restrain using Becke's three-parameter hybrid exchange functional (B3) and the Lee-Yang-Parr correlation functional (LYP) (B3LYP) along with 6-31g(d) basis set [30-34]. The GaussView 5.0.8 program was used for the images of optimized structures and the energy levels of highest occupied molecular orbital (HOMO)-lowest unoccupied molecular orbital (LUMO). The calculated structures of probe **FLPG** and its complexes (**FLPG**-Cu^{2+} and **FLPG**-Fe^{3+}) were illustrated in Fig. **6**. As seen in Fig. **6**, the electrons were fundamentally localized on the triazine moiety in free probe **FLPG**, while the electrons were mainly localized on Cu^{2+} or Fe^{3+} in the complex forms. These outcomes are attributed to the charge transfer (LMCT) from the probe **FLPG** moiety to the target metal ions. As well, as a result of the formation of stable complexes **FLPG**-Cu^{2+} and **FLPG**-Fe^{3+}, the band gaps between the HOMO and LUMOs of probe **FLPG** (4.99 eV) were lowered after the complexation with Cu^{2+} (1.21 eV) and Fe^{3+} (2.81), which show the structure of a stable complex and the high affinity of probe **FLPG** towards Cu^{2+} or Fe^{3+}.

3.5. Living-cell Studies

Cytotoxic properties of the probe **FLPG**, Cu^{+2} and Fe^{+3} ions on HepG2 cells are summarized in Fig. **S9a-c**. According to the results, the probe **FLPG** and metal ions demonstrated cytotoxic effects with increasing concentrations separately. Especially after 50 μM applications, cell viability decreased drastically. For the 24-h incubation, the dose of the probe that reduced the cell viability at 50% (IC_{50} values) was calculated as 35.18 ± 1.09 μM. Additionally, cupric and ferric ions also demonstrated cytotoxic effects (IC_{50}: 48.14 ± 1.21 and 57.43 ±1.15 for Cu^{+2} and Fe^{+3}, respectively) as incubated for 24-hrs. On the other hand, it is important to note that our cytotoxicity tests and *in vitro* imaging studies (Fig. **7**)

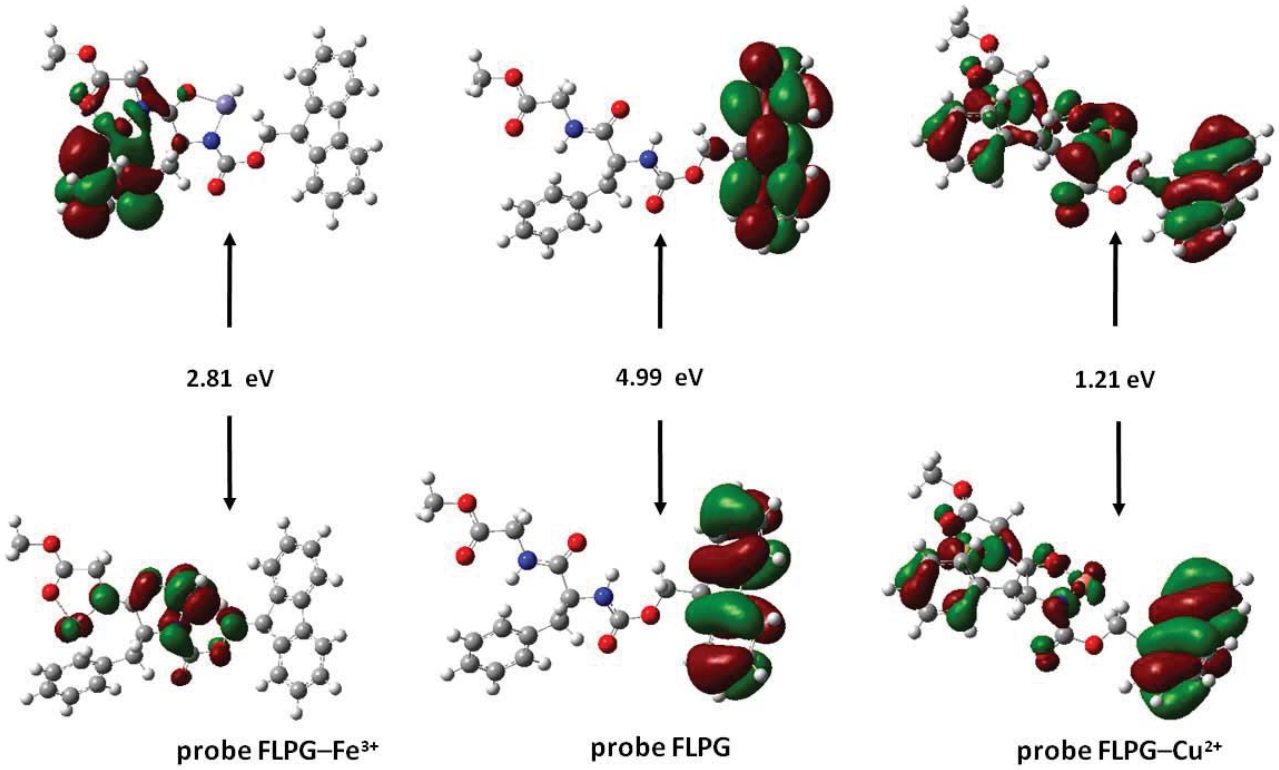

Fig. (6). Frontier molecular orbitals and HOMO-LUMO energy level diagrams of probe **FLPG** and its complexes of **FLPG-Cu^{2+}** and **FLPG-Fe^{3+}**. (*A higher resolution / colour version of this figure is available in the electronic copy of the article*).

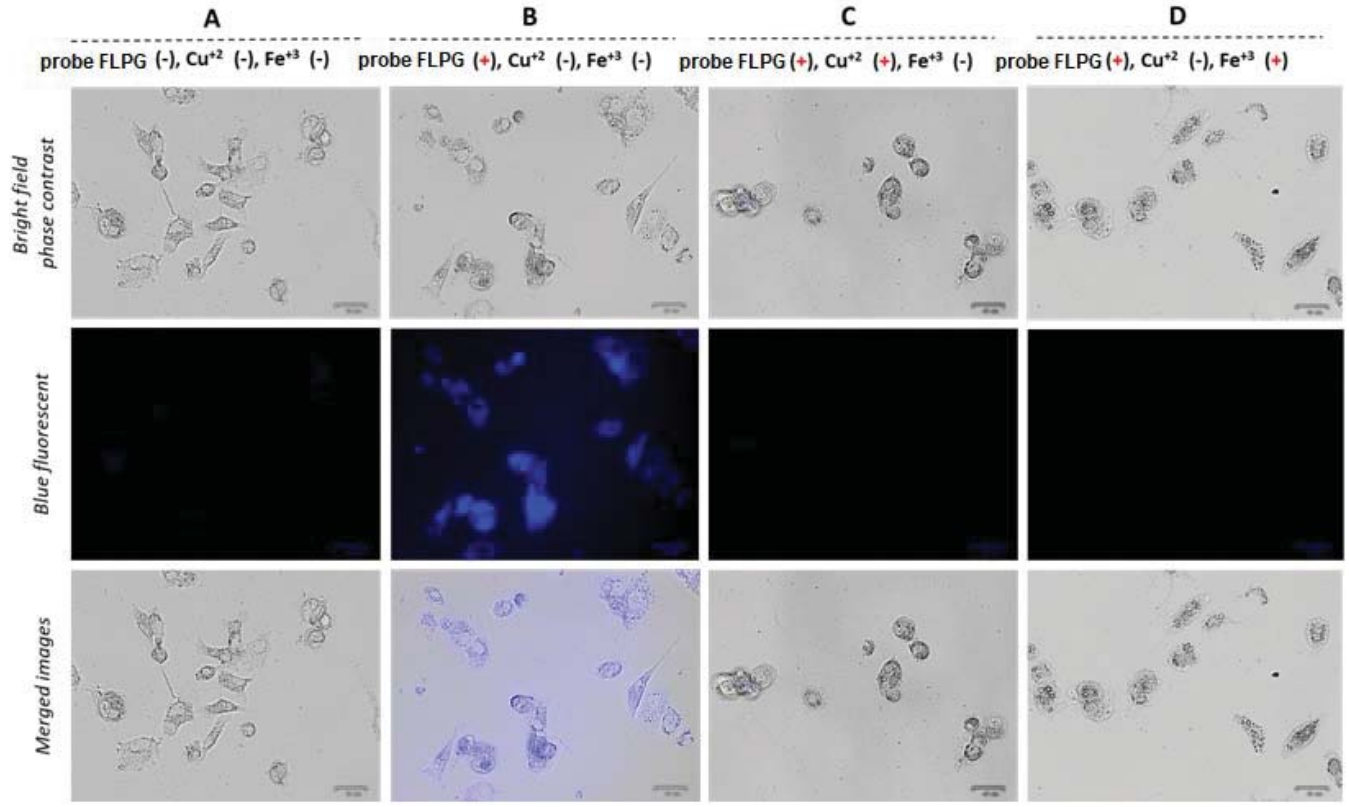

Fig. (7). Bright-field, **(a)** blue fluorescence and merged images of HepG2 cells alone, **(b)** treated with only 50 μM probe **FLPG**, **(c)** treated with 50 μM probe **FLPG** and then 50 μM Cu^{+2}, **(d)** treated with 50 μM probe **FLPG** and then 50 μM Fe^{+3}. Images were taken with a fluorescent cell imaging system (ZOE, Bio-Rad, λex = 355/40 nm, λem = 433/36 nm). Scale bars represent the 40 μm length. (*A higher resolution / colour version of this figure is available in the electronic copy of the article*).

also demonstrated any significant cytotoxic effects of 50 μM probe and metal ions for one-hour incubation over the HepG2 cells.

The results of fluorescent cell imaging studies are summarized in Fig **7**. As demonstrated in Fig. **7a** and **7b**, the probe **FLPG** alone increased the intracellular blue fluorescence in HepG2 cells, suggesting that it could penetrate cellular membranes and be effective in intracellular imaging applications. On the other hand, if the cells were treated with Cu^{+2} and Fe^{+3} ions separately after the probe **FLPG** treatment, a dramatic decrease in intracellular blue fluorescence was observed (Fig. **7c-7d**). These results demonstrate the diffusion of these metal ions into the cells and the quenching ability of the probe **FLPG** fluorescence.

CONCLUSION

In summary, we have successfully designed, synthesized and characterized a fluorene-based fluorogenic chemosensor, which is highly selective and sensitive for Cu^{2+} and Fe^{3+} detection in CH_3CN/HEPES (9/1, v/v, pH=7.4) media. The probe **FLPG** has quite lower detection limits for Cu^{2+} (25.07 nM) and Fe^{3+} (37.80 nM), as well as high selectivities. The binding constants with strongly interacting Cu^{2+} and Fe^{3+} were determined as 4.56×10^{8} M^{-2} and 2.02×10^{10} M^{-2}, respectively, *via* the fluorescence titration experiments. The outcomes of the computational study supported the fluorescence data. Moreover, the practical application of the probe **FLPG** was successfully performed for a living-cells. Therefore, this simple chemosensor system offers a highly selective and sensitive sensing platform for the routine detection of Cu^{2+} and Fe^{3+}, and it keeps away from the usage of costly and sophisticated analysis systems.

ETHICS APPROVAL AND CONSENT TO PARTICIPATE

Not applicable.

HUMAN AND ANIMAL RIGHTS

No animals/humans were used in this study.

CONSENT FOR PUBLICATION

Not applicable.

AVAILABILITY OF DATA AND MATERIALS

The data supporting the findings of this study are available within the article and/ its supplementary materials.

FUNDING

None.

CONFLICT OF INTEREST

We declare that we have no known competing financial interests or personal relationships that could have appeared to influence the work reported in this study.

ACKNOWLEDGEMENTS

The authors are grateful to the KMU for their support (project numbers 13-YL-18 and 30-M-16) and providing the Gaussian-09 database and GaussView-5.0.8 software.

SUPPLEMENTARY MATERIAL

Supplementary material is available on the publisher's website along with the published article.

REFERENCES

[1] Li, D.; Sun, Y.; Shen, Q.; Zhang, Q.; Huang, W.; Kang, Q.; Shen, D. Smartphone-based three-channel ratiometric fluorescent device and application in filed analysis of Hg^{2+}, Fe^{3+} and Cu^{2+} in water samples. *Microchem. J.,* **2020**, *152*, 104423. http://dx.doi.org/10.1016/j.microc.2019.104423

[2] Wang, S.; Cong, T.; Liang, Q.; Li, Z.; Xu, S. Dual colorimetric and fluorescent chemosensor of Fe^{3+} and Cu^{2+} croconine. *Tetrahedron,* **2015**, *71*, 5478-5483. http://dx.doi.org/10.1016/j.tet.2015.06.081

[3] Weerasinghe, A.J.; Abebe, F.A.; Sinn, E. Rhodamine based turn-on dual sensor for Fe^{3+} and Cu^{2+}. *Tetrahedron Lett.,* **2011**, *52*, 5648-5651. http://dx.doi.org/10.1016/j.tetlet.2011.08.092

[4] Elif, Ş.; Bingul, M.; Saglam, M.F.; Kandemir, H.; Sengul, I.F. Synthesis of a novel N,N′,N′-tetraacetyl-4,6-dimethoxyindole-based dual chemosensor for the recognition of Fe^{3+} and Cu^{2+} ions. *Inorg. Chim. Acta,* **2019**, *495*, 118947. http://dx.doi.org/10.1016/j.ica.2019.05.046

[5] Chen, Z.E.; Zang, X.F.; Yang, M.; Zhang, H. A simple indolo[2,3-a]carbazole based colorimetric chemosensor for simultaneous detection of Cu^{2+} and Fe^{3+} ions. *Spectrochim. Acta A Mol. Biomol. Spectrosc.,* **2020**, *234*, 118236. http://dx.doi.org/10.1016/j.saa.2020.118236 PMID: 32179460

[6] Erdemir, S.; Malkondu, S.; Kocyigit, O.A. Blue / red dual-emitting multi-responsive fluorescent Probe for Fe^{3+}, Cu^{2+} and cysteine based on isophorone-antharecene. *Microchem. J.,* **2020**, *157*, 105075. http://dx.doi.org/10.1016/j.microc.2020.105075

[7] Wang, J.; Wei, T.; Ma, F.; Li, T.; Niu, Q. A novel fluorescent and colorimetric dual-channel sensor for the fast, reversible and simultaneous detection of Fe^{3+} and Cu^{2+} based on terthiophene derivative with high sensitivity and selectivity. *J. Photochem. Photobiol. Chem.,* **2019**, *383*, 111982. http://dx.doi.org/10.1016/j.jphotochem.2019.111982

[8] Joshi, S.; Kumari, S.; Sarmah, A.; Sakhuja, R.; Pant, D.D. Solvatochromic shift and estimation of dipole moment of synthesized coumarin derivative: Application as sensor for fluorogenic recognition of Fe^{3+} and Cu^{2+} ions in aqueous solution. *J. Mol. Liq.,* **2016**, *222*, 253-262. http://dx.doi.org/10.1016/j.molliq.2016.07.047

[9] Guo, Y.; Wang, L.; Zhuo, J.; Xu, B.; Li, X.; Zhang, J.; Zhang, Z.; Chi, H.; Dong, Y.; Lu, G. A pyrene-based dual chemosensor for colorimetric detection of Cu^{2+} and fluorescent detection of Fe^{3+}. *Tetrahedron Lett.,* **2017**, *58*, 3951-3956. http://dx.doi.org/10.1016/j.tetlet.2017.08.078

[10] Desai, V.; Kaler, S.G. Role of copper in human neurological disorders. *Am. J. Clin. Nutr.,* **2008**, *88*(3), 855S-858S. http://dx.doi.org/10.1093/ajcn/88.3.855S PMID: 18779308

[11] Brewer, G.J. Iron and copper toxicity in diseases of aging, particularly atherosclerosis and Alzheimer's disease. *Exp. Biol. Med. (Maywood),* **2007**, *232*(2), 323-335. PMID: 17259340

[12] Lal, S.; Kumar, S.; Hooda, S.; Kumar, P. A highly selective sensor for Cu^{2+} and Fe^{3+} ions in aqueous medium: Spectroscopic, computational and cell imaging studies. *J. Photochem. Photobiol. Chem.,* **2018**, *364*, 811-818.

http://dx.doi.org/10.1016/j.jphotochem.2018.07.021

[13] Myint, Z.W.; Oo, T.H.; Thein, K.Z.; Tun, A.M.; Saeed, H. Copper deficiency anemia: review article. *Ann. Hematol.,* **2018**, *97*(9), 1527-1534.
http://dx.doi.org/10.1007/s00277-018-3407-5 PMID: 29959467

[14] Klevay, L.M. Trace element nutrition and human health cardiovascular disease from copper deficiency-a history. *J. Nutr.,* **2000**, *130*, 489-492.
http://dx.doi.org/10.1093/jn/130.2.489S

[15] Şenkuytu, E. A high selective turn-off aminopyrene based cyclotriphosphazene fluorescent chemosensors for Fe^{3+} Cu^{2+} ions. *Inorg. Chim. Acta,* **2018**, *479*, 58-65.
http://dx.doi.org/10.1016/j.ica.2018.04.028

[16] Li, S.; Zhang, D.; Xie, X.; Ma, S.; Liu, Y.; Xu, Z.; Gao, Y. A novel solvent-dependently bifunctional NIR absorptive and fluorescent ratiometric probe for detecting Fe^{3+}/Cu^{2+} and its application in bioimaging. *Sens. Actuators B Chem.,* **2016**, *224*, 661-667.
http://dx.doi.org/10.1016/j.snb.2015.10.086

[17] Yang, Y.; Gao, C.; Zhang, N.; Dong, D. Tetraphenylethene functionalized rhodamine chemosensor for Fe^{3+} and Cu^{2+} ions in aqueous media. *Sens. Actuators B Chem.,* **2016**, *222*, 741-746.
http://dx.doi.org/10.1016/j.snb.2015.08.125

[18] Altamura, S.; Muckenthaler, M.U. Iron toxicity in diseases of aging: Alzheimer's disease, Parkinson's disease and atherosclerosis. *J. Alzheimers Dis.,* **2009**, *16*(4), 879-895.
http://dx.doi.org/10.3233/JAD-2009-1010 PMID: 19387120

[19] Wood, J.C.; Ghugre, N. Magnetic resonance imaging assessment of excess iron in thalassemia, sickle cell disease and other iron overload diseases. *Hemoglobin,* **2008**, *32*(1-2), 85-96.
http://dx.doi.org/10.1080/03630260701699912 PMID: 18274986

[20] Qian, Z.M.; Wang, Q. Expression of iron transport proteins and excessive iron accumulation in the brain in neurodegenerative disorders. *Brain Res. Brain Res. Rev.,* **1998**, *27*(3), 257-267.
http://dx.doi.org/10.1016/S0165-0173(98)00012-5 PMID: 9729418

[21] Çukurovali, A.; Yilmaz, I.; Özmen, H. Antimicrobial Activity Studies of the Metal Complexes Derived from Substituted Cyclobutane Substituted Thiazole Schiff Base Ligands. *Transit. Met. Chem.,* **2001**, *26*, 619-624.
http://dx.doi.org/10.1023/A:1012006404144

[22] Cukurovali, A.; Yilmaz, I. Synthesis and characterization of a new cyclobutane substituted schiff base ligand and its Cd(II), Co(II), Ni(II) and Zn(II) complexes. *Pol. J. Chem.,* **2000**, *74*, 147-151.
http://dx.doi.org/10.1002/chin.200023130

[23] Aksuner, N.; Henden, E.; Yilmaz, I.; Cukurovali, A. Development of a highly sensitive and selective optical chemical sensor for the determination of zinc based on fluorescence quenching of a novel schiff base ligand. *Sens. Lett.,* **2010**, *8*, 684-689.
http://dx.doi.org/10.1166/sl.2010.1330

[24] Aksuner, N.; Henden, E.; Yenigul, B.; Yilmaz, I.; Cukurovali, A. Highly sensitive sensing of zinc(II) by development and characterization of a PVC-based fluorescent chemical sensor. *Spectrochim. Acta A Mol. Biomol. Spectrosc.,* **2011**, *78*(3), 1133-1138.
http://dx.doi.org/10.1016/j.saa.2010.12.065 PMID: 21257342

[25] Karuk Elmas, Ş.N.; Ozen, F.; Koran, K.; Yilmaz, I.; Gorgulu, A.O.; Erdemir, S. Coumarin Based Highly Selective "off-on-off" Type Novel Fluorescent Sensor for Cu^{2+} and S^{2-} in Aqueous Solution. *J. Fluoresc.,* **2017**, *27*(2), 463-471.
http://dx.doi.org/10.1007/s10895-016-1972-3 PMID: 27995460

[26] Wang, J.; Wei, T.; Ma, F.; Li, T.; Niu, Q. A novel fluorescent and colorimetric dual-channel sensor for the fast, reversible and simultaneous detection of Fe^{3+} and Cu^{2+} based on terthiophene derivative with high sensitivity and selectivity. *J. Photochem. Photobiol. Chem.,* **2019**, 383.
http://dx.doi.org/10.1016/j.jphotochem.2019.111982

[27] Kawakami, J.; Sasaki, Y.; Yanase, K.; Ito, S. Benzo-fused BODIPY derivative as a fluorescent chemosensor for Fe^{3+}, Cu^{2+}, and Al^{3+}. *Trans. Mater. Res. Soc. Jpn.,* **2019**, *73*, 3-7.
http://dx.doi.org/10.14723/tmrsj.44.69

[28] Zhang, B.; Liu, H.; Wu, F.; Hao, G.F.; Chen, Y.; Tan, C.; Tan, Y.; Jiang, Y. A dual-response quinoline-based fluorescent sensor for the detection of copper (II) and iron(III) ions in aqueous medium. *Sens. Actuators B Chem.,* **2017**, *243*, 765-774.
http://dx.doi.org/10.1016/j.snb.2016.12.067

[29] Zhu, X.; Duan, Y.; Li, P.; Fan, H.; Han, T.; Huang, X. A highly selective and instantaneously responsive schiff base fluorescent sensor for the "turn-off" detection of iron(III), iron(II), and copper(II) ions. *Anal. Methods,* **2019**, *11*, 642-647.
http://dx.doi.org/10.1039/C8AY02526F

[30] Hay, P.J.; Wadt, W.R.; Hay, P.J.; Wadt, W.R. Ab initio effective core potentials for molecular calculations. potentials for the transition metal atoms Sc to Hg Ab initio effective core potentials for molecular calculations. potentials for the transition metal atoms Sc to Hg. *J. Chem. Phys.,* **1985**, *82*(1), 270-283.
http://dx.doi.org/10.1063/1.448799

[31] Lee, C.; Hill, C.; Carolina, N. Development of the colic-salvetti correlation-energy formula into a functional of the electron density. *Phys. rewiev B,* **1988**, *37*, 785-789.

[32] Becke, A.D. Becke's three parameter hybrid method using the LYP correlation functional. *J. Chem. Phys.,* **1993**, *98*, 5648-5652.
http://dx.doi.org/10.1063/1.464913

[33] Frisch, A.M.J.; Trucks, G.W.; Schlegel, H.B.; Scuseria, G.E.; Robb, M.A.; Cheeseman, J.R.; Scalmani, G.; Barone, V. *09 Revision D.01,* **2014**.

[34] Dennington, R.; Keith, T.A.; Millam, J.M. *GaussView Version 5,* **2009**.

[35] Garrett, C.E.; Jiang, X.; Prasad, K.; Repic, O. New Observations on Peptide Bond Formation Using CDMT. *Tetrahedron Lett.,* **2002**, *43*, 4161-4165.
http://dx.doi.org/10.1016/S0040-4039(02)00754-2

[36] Percec, V.; Dulcey, A.E.; Peterca, M.; Adelman, P.; Samant, R.; Balagurusamy, V.S.K.; Heiney, P.A.; Uni, V.; Pennsyl, V. Helical pores self-assembled from homochiral dendritic dipeptides based on L-Tyr and nonpolar alpha-amino acids. *J. Am. Chem. Soc.,* **2007**, *129*(18), 5992-6002.
http://dx.doi.org/10.1021/ja071088k PMID: 17429976

[37] Shi, Y.; Ye, J.; Qi, Y.; Akram, M.A.; Rauf, A.; Ning, G. An anionic layered europium(iii) coordination polymer for solvent-dependent selective luminescence sensing of Fe^{3+} and Cu^{2+} ions and latent fingerprint detection. *Dalton Trans.,* **2018**, *47*(48), 17479-17485.
http://dx.doi.org/10.1039/C8DT04042G PMID: 30511078

[38] Qiu, S.; Cui, S.; Shi, F.; Pu, S. Novel diarylethene-based fluorescent switching for the detection of Al^{3+} and construction of logic circuit. *ACS Omega,* **2019**, *4*(12), 14841-14848.
http://dx.doi.org/10.1021/acsomega.9b01432 PMID: 31552323

[39] Aydin, D. A novel turn on fluorescent probe for the determination of Al^{3+} and Zn^{2+} ions and its cells applications. *Talanta,* **2020**, *210*, 120615.
http://dx.doi.org/10.1016/j.talanta.2019.120615 PMID: 31987182

[40] Phapale, D.; Gaikwad, A.; Das, D. Selective recognition of Cu (II) and Fe (III) using a pyrene based chemosensor. *Spectrochim. Acta A Mol. Biomol. Spectrosc.,* **2017**, *178*, 160-165.
http://dx.doi.org/10.1016/j.saa.2017.01.064 PMID: 28182986

[41] Dos Santos Carlos, F.; Monteiro, R.F.; da Silva, L.A.; Zanlorenzi, C.; Nunes, F.S. A highly selective acridine-based fluorescent probe for detection of Al^{3+} in alcoholic beverage samples. *Spectrochim. Acta A Mol. Biomol. Spectrosc.,* **2020**, *231*, 118119.
http://dx.doi.org/10.1016/j.saa.2020.118119 PMID: 32032858

[42] Nunes, M.C.; Carlos, F. dos S.; Fuganti, O.; Galindo, D.D.; De Boni, L.; Abate, G.; Nunes, F.S. Turn-on fluorescence study of a highly selective acridine-based chemosensor for Zn2+ in aqueous solutions. *Inorg. Chim. Acta,* **2020**, *499*, 119191.
http://dx.doi.org/10.1016/j.ica.2019.119191

[43] Jiang, Z.; Tang, L.; Shao, F.; Zheng, G.; Lu, P. Synthesis and characterization of 9-(cycloheptatrienylidene)fluorene derivatives: New fluorescent chemosensors for detection of Fe^{3+} and Cu^{2+}. *Sens. Actuators B Chem.,* **2008**, *134*, 414-418.
http://dx.doi.org/10.1016/j.snb.2008.05.019

[44] Cheng, P.; Xu, K.; Yao, W.; Xie, E.; Liu, J. Novel fluorescent chemosensors based on carbazole for Cu^{2+} and Fe^{3+} in aqueous media. *J. Lumin.,* **2013**, *143*, 583-586. http://dx.doi.org/10.1016/j.jlumin.2013.06.013

[45] Wang, L.; Ye, D.; Li, W.; Liu, Y.; Li, L.; Zhang, W.; Ni, L. Fluorescent and colorimetric detection of Fe(III) and Cu(II) by a difunctional rhodamine-based probe. *Spectrochim. Acta A Mol. Biomol. Spectrosc.,* **2017**, *183*, 291-297. http://dx.doi.org/10.1016/j.saa.2017.04.056 PMID: 28456087

[46] Huang, C.Y. Determination of binding stoichiometry by the continuous variation method: the Job plot. *Methods Enzymol.,* **1982**, *87*, 509-525. http://dx.doi.org/10.1016/S0076-6879(82)87029-8 PMID: 7176926